MATHEMATICAL MODELING OF THE DIFFUSION OF WATER IN WOOD DURING DRYING

Kirk C. Nadler
Graduate Student
Department of Chemical Engineering

Elvin T. Choong
Professor
School of Forestry, Wildlife, and Fisheries

and

David M. Wetzel
Associate Professor
Department of Chemical Engineering
Louisiana State University, Baton Rouge, LA 70803

(Received May 1984)

ABSTRACT

The drying of lumber was modeled by the diffusion of water in wood, according to Fick's second law. In the model the following assumptions were made: (1) Moisture content is the driving force; (2) the diffusion coefficient is a constant value above the fiber saturation point and one-fourth that value below the fiber saturation point; (3) equilibrium exists between the moisture content at the wood surface and the film of air adjacent to the surface; (4) moisture movement from the film to the bulk air stream occurs by film mass transfer. Five independent variables—half thickness of the board, species factor (density-diffusivity), temperature, relative humidity, and air velocity—were found to influence the drying process. This study reveals that variable interactions are important considerations when one wishes to predict drying times.

Using red oak and constant values for lumber thickness and kiln air velocity, three cases were modeled to illustrate the potential for improved operation. The first case follows temperature and humidity schedules typical of current kiln operations, forming a basis for comparison. In the second case, a solar-powered kiln produces harmonic variations in temperature and relative humidity. The most favorable drying conditions occur in the late afternoon, the least favorable before dawn. Slower drying with nightly relaxation of the moisture profile may produce a board with few defects. In the final study, temperature and maximum permissible drying rate are specified, with relative humidity chosen according to the model. This case produced the most rapid drying, yet has milder moisture gradients than the base case. The results of these studies show the possibility of producing a high-quality product at low cost in a solar-powered dryer, or optimizing drying schedules to reduce drying time and increase product quality.

Keywords: Kiln drying, diffusion, air velocity, humidity, solar power.

INTRODUCTION

The drying technology of wood is largely an art rather than a science, because fundamental knowledge about the wood-drying process is still lacking. Most studies have dealt with either the external factors affecting the evaporation of moisture from the wood surface or with the internal factors causing the moisture to move from the wood interior to the surface. In moisture movement, most studies have centered on the hygroscopic moisture, which represents a small portion of the

Wood and Fiber Science, 17(3), 1985, pp. 404–423

entire moisture range. Thus, moisture movement during drying has been largely expressed in terms of a diffusion phenomenon below the fiber saturation point. The mechanism of free water movement in the void structure is still not well understood.

The diffusion coefficient for water in wood has been determined from drying data at fixed boundary conditions by numerous researchers (Skaar 1954; Bigger-staff 1965; Stamm and Nelson 1961; Choong 1963; McNamara and Hart 1971; Bui et al. 1980) using the general solution of Fick's second law given by Newman (1931). These studies, however, have not considered the effect of surface resistance, which was reported by Ogura (1950) and by Choong and Skaar (1972) to be significant for samples less than 1.2 in. in thickness. Surface resistance can also be expected to be pronounced when there is inadequate air circulation, especially during the beginning of drying.

This study was undertaken to investigate the wood drying process as a mass transfer problem. Drying of wood is modeled by the equation for unsteady-state diffusion. For the solution of the equation, boundary conditions were chosen to resemble those existing in a dry kiln, with several important variables taken into consideration in order to simulate various drying conditions.

Several drying simulations have been reported in the literature. Peck and Kauh (1969) report average values of concentration based on a uniform mass diffusivity, with vapor pressure on the surface as the surface boundary condition. Ashworth (1980) uses a temperature-dependent diffusivity and a surface boundary condition based on heat transfer analogies. Spolek and Plumb (1980) base their model on capillary action above fiber saturation and diffusion below fiber saturation. In this study, we assumed the surface concentration of vapor is given by the adsorption equilibrium relationship. We also assumed an isothermal condition in the wood and a two-part diffusion coefficient.

DEVELOPMENT OF THE MODEL

Fick's second law,

$$\frac{\partial C_{H_2O}}{\partial t} = D\frac{\partial^2 C_{H_2O}}{\partial Z^2}, \tag{1}$$

has often been used to describe the unsteady-state, one-dimensional movement of moisture through wood. In this equation, C_{H_2O} is the concentration of water in the wood (mass water/volume green wood), D is the diffusion coefficient (area/time), t is the time, and Z is the distance from the center of the board.

We concur with the literature (Bateman et al. 1939; Stamm 1964; Hart 1964) that diffusion controls the entire range of moisture content during the drying of wood below the boiling point of water. Thus drying can be accurately modeled as a diffusion phenomenon. This is applicable whether the movement of moisture involves only the bound water and water vapor forms, or includes the free water form as well. It is especially true in a moderately impermeable hardwood, where the mass flow of free water is restricted. We have chosen to use Fick's law to model moisture movement both above and below the fiber saturation point and have done so by the incorporation of a two-part diffusion coefficient. The diffusion

coefficient is represented by a high constant value when the moisture content is above the fiber saturation point and a low constant value when below the fiber saturation point.

The effect of moisture content on diffusion coefficient is still controversial. In the steady-state movement, the diffusion coefficient increases exponentially with moisture content in the hygroscopic range, while the unsteady-state results have been conflicting (Hart 1964; Moschler and Martin 1968; Bui et al. 1980). The diffusion coefficient is likely to be constant above the fiber saturation point because the humidity inside the wood is near saturation. Below the fiber saturated point, we can expect the change in diffusion coefficient with moisture content to be minimal if we deal with small changes in humidity. For these reasons, we used two diffusion coefficient values and two humidity values.

We assumed isothermal conditions in our model because the diffusivity of heat is much greater than the diffusivity of mass. (The Lewis number is large.) After a change in kiln temperature, isothermal conditions in the board are reestablished rapidly compared to time scale of the diffusion process. Even if a small temperature gradient exists within the board, it will not significantly affect the diffusion coefficient. Biggerstaff (1965), working with 0.25-in.-thick samples, found almost the same diffusion coefficient in boards preheated to kiln temperatures of 50 C, 70 C, and 90 C, and boards initially at room temperature. Choong (1965) reported that over the temperature range 40–60 C, diffusion coefficients are independent of temperature.

We can partly non-dimensionalize Eq. (1) by introducing the new variables $X = Z/L$ and $M = C_{H_2O}/\rho_{wood}$, where L is the half-thickness of the board, and X is the dimensionless distance from the centerline, ρ_{wood} is the wood density (mass dry wood/volume green wood), M is the dimensionless moisture content (mass water/mass dry wood). To solve the resulting equation,

$$\frac{\partial M}{\partial t} = \frac{D}{L^2}\frac{\partial^2 M}{\partial X^2}, \tag{2}$$

we need an initial condition and two boundary conditions.

The initial condition is given by:

$$M = M_0 \quad \text{at} \quad t = 0, \qquad \text{all } X, \tag{3}$$

which describes an initially constant moisture content throughout the board.

One boundary condition is given by:

$$\frac{\partial M}{\partial X} = 0 \quad \text{at} \quad X = 0, \qquad \text{all } t, \tag{4}$$

which describes a symmetrical moisture profile located along the centerline of the board.

The second boundary condition accounts for the surface resistance to mass transfer. This is found by equating the moisture flux toward the board surface by internal diffusion to the moisture flux away from the board surface by convection into the bulk air stream:

$$-D\frac{\partial C_{H_2O}}{\partial Z}\bigg|_{Z=L} = K_c(C_{surf} - C_{bulk}). \quad (5)$$

In this equation, C_{surf} and C_{bulk} are the water vapor densities at the board surface and in the bulk air stream (mass/volume), and K_c is the external mass transfer coefficient (length/time). After multiplying Eq. (5) by $L/D\rho_{wood}$, using the ideal gas law to express the water vapor densities in terms of partial pressures, and noting that the relative humidity is the ratio of the partial pressure of water to its vapor pressure, we arrive at the edge boundary condition:

$$\frac{-\partial M}{\partial X}\bigg|_{X=1} = \frac{Sh}{\rho_{wood}}\frac{P_{sat}M_w}{RT}(RH_{surf} - RH_{bulk}). \quad (6)$$

where Sh is the Sherwood number (K_cL/D), M_w is the molecular weight of water, T is the absolute temperature, R is the gas constant, P_{sat} is the saturated water vapor pressure, and RH_{surf} and RH_{bulk} are the relative humidities of the air at the board surface and in the bulk air stream.

We can relate RH_{surf} to the wood moisture content at the surface by means of a suitable sorption isotherm. Relative humidity–temperature–equilibrium moisture content data in the Wood Handbook (Forest Product Laboratory 1974) were fitted to the following function:

$$M_e = C_1 + C_2RH_{surf} + C_3RH_{surf}^2 + C_4RH_{surf}^3 + C_5T + C_6RH_{surf}T + C_7/T, \quad (7)$$

where M_e is the equilibrium moisture content, and the constants, determined by linear least squares regression, are: $C_1 = 1.2969$, $C_2 = 36.6069$, $C_3 = -53.5160$, $C_4 = 45.9798$, $C_5 = -1.2245 \times 10^{-2}$, $C_6 = -3.5224 \times 10^{-2}$, and $C_7 = -53.7984$.

Equation (2) with initial condition (3) and boundary conditions (4) and (6)–(7) was solved in finite difference form using the Crank-Nicholson technique. The presence of Eq. (7) makes the surface boundary condition nonlinear. Nadler (1983) discusses the solution technique in detail.

Five independent variables were identified that affected the drying model: half-thickness, species factor, temperature, relative humidity, and air velocity. In order to investigate all possible combinations of these variables, we used a two-level factorial design (Box et al. 1978). In a factorial design, two typical values, one high and one low, are chosen for each of the five variables, resulting in 2^5 or 32 solutions of the model equations.

Four of the variables can be controlled by the kiln operator: board thickness, temperature, relative humidity, and air velocity. The fifth variable is called the species factor because it contains the wood density and diffusivity, which are determined by the choice of wood species. The species factor treats density and diffusivity as a single variable, because density and diffusivity of a species are interdependent. However, the drying rate cannot be modeled by using density or diffusivity alone. These values are listed in Table 1. Those chosen for thickness, temperature, relative humidity, and air velocity are high and low values commonly found in hardwood kilns (Greenhill 1936; Keer 1956; Rosen 1978; Salamon 1960; Vick 1956).

TABLE 1. *Values of the independent variables.*

Variable	(+) Value	(−) Value	Units
A) Half-thickness	0.0625	0.0417	ft
B) Species factor			
Density (oven dried weight, green volume)	43.0	28.0	lb/ft^3
High diffusivity	1.7×10^{-6}	5.0×10^{-6}	cm^2/sec
Low diffusivity	0.43×10^{-6}	1.25×10^{-6}	cm^2/sec
C) Temperature	130.0	90.0	°F
D) Relative humidity	0.95	0.60	fraction
E) Air velocity	600	200	ft/min

The values chosen for the species-factor-dependent variables were calculated from experimental data and from relationships in the literature. The more dense board is chosen to resemble a moderately heavy hardwood, such as red oak, which has a density of about 43 lb/ft^3 (690 kg/m^3), based on oven-dry weight and green volume.

The equation:

$$D = \frac{\pi L^2}{4t}\left(\frac{M_0 - \bar{M}}{M_0 - M_e}\right)^2, \tag{8}$$

can be derived and has been used to determine the diffusion coefficient during drying. In it M_0 is the initial moisture content, $\bar{M}$ the average moisture content, and M_e the equilibrium moisture content. The diffusion coefficient of 1.7×10^{-6} cm^2/sec was calculated with Eq. (8), using experimental data produced at the LSU School of Forestry and Wildlife Management for the transverse movement of moisture above the fiber saturation point in red oak (Mamit 1983).

For the less dense species, the diffusion coefficient above the fiber saturation point was taken to be 5×10^{-6} cm^2/sec. This number was estimated by noting that as the density decreases, the amount of cell wall decreases. Thus, bound water diffusion through and along the surface of the cell walls is less important than for dense species. Also, the area available for vapor diffusion through the lumens becomes larger and less tortuous than for dense species, so that the effective diffusivity is increased. With these facts in mind, it was estimated that the diffusion coefficients in the less dense species are about three times higher than those in the more dense species (Yao 1966).

An equation presented by Moschler and Martin (1968) expressing D as a function of moisture content was used to estimate the ratio of the diffusivities above and below the fiber saturation point. Their equation is for yellow poplar, but it is assumed that the functional form is valid for both species considered in this study. The equation

$$D = [5.2 - 1.2\,(100M) + 0.08\,(100M)^2] \times 10^{-6} \tag{9}$$

shows that as the moisture content rises from 0.2 lb water/lb dry wood to the fiber saturation point, the diffusion coefficient increases by a factor of about four.

TABLE 2. *Simulated drying time to reach average moisture content of 0.3 lb water/lb dry wood under indicated conditions. (The plus or minus signs refer to the corresponding values in Table 1.)*

Drying run	Variable					Time (hours) to M = 0.3
	A	B	C	D	E	
1	−	−	−	−	−	53
2	+	−	−	−	−	120
3	−	+	−	−	−	156
4	+	+	−	−	−	345
5	−	−	+	−	−	50
6	+	−	+	−	−	112
7	−	+	+	−	−	146
8	+	+	+	−	−	330
9	−	−	−	+	−	195
10	+	−	−	+	−	322
11	−	+	−	+	−	358
12	+	+	−	+	−	659
13	−	−	+	+	−	90
14	+	−	+	+	−	183
15	−	+	+	+	−	231
16	+	+	+	+	−	508
17	−	−	−	−	+	52
18	+	−	−	−	+	116
19	−	+	−	−	+	153
20	+	+	−	−	+	345
21	−	−	+	−	+	50
22	+	−	+	−	+	112
23	−	+	+	−	+	146
24	+	+	+	−	+	330
25	−	−	−	+	+	129
26	+	−	−	+	+	233
27	−	+	−	+	+	280
28	+	+	−	+	+	578
29	−	−	+	+	+	80
30	+	−	+	+	+	173
31	−	+	+	+	+	225
32	+	+	+	+	+	501

A = half-thickness; B = species factor; C = temperature; D = relative humidity; E = air velocity.

Using this factor we estimated the diffusion coefficient of yellow poplar below fiber saturation to be about 1.25×10^{-6} cm^2/sec, and of red oak to be 0.43×10^{-6} cm^2/sec.

All computer runs assumed the initial moisture profile was constant at 1.0 lb water/lb dry wood, the fiber saturation point was 0.3 lb water/lb dry wood, and the equilibrium moisture content is below fiber saturation.

RESULTS AND DISCUSSION

Before working out several case studies, we chose as a base study the calculation of the time required to dry a board from its initial moisture content down to an average moisture content of 0.3 lb water/lb dry wood. Under the high humidity condition in the factorial design study, the equilibrium moisture content is 0.28. This precluded choosing a lower, and more realistic, final moisture content as it would not cover all the cases in the base study. However, the model is valid to

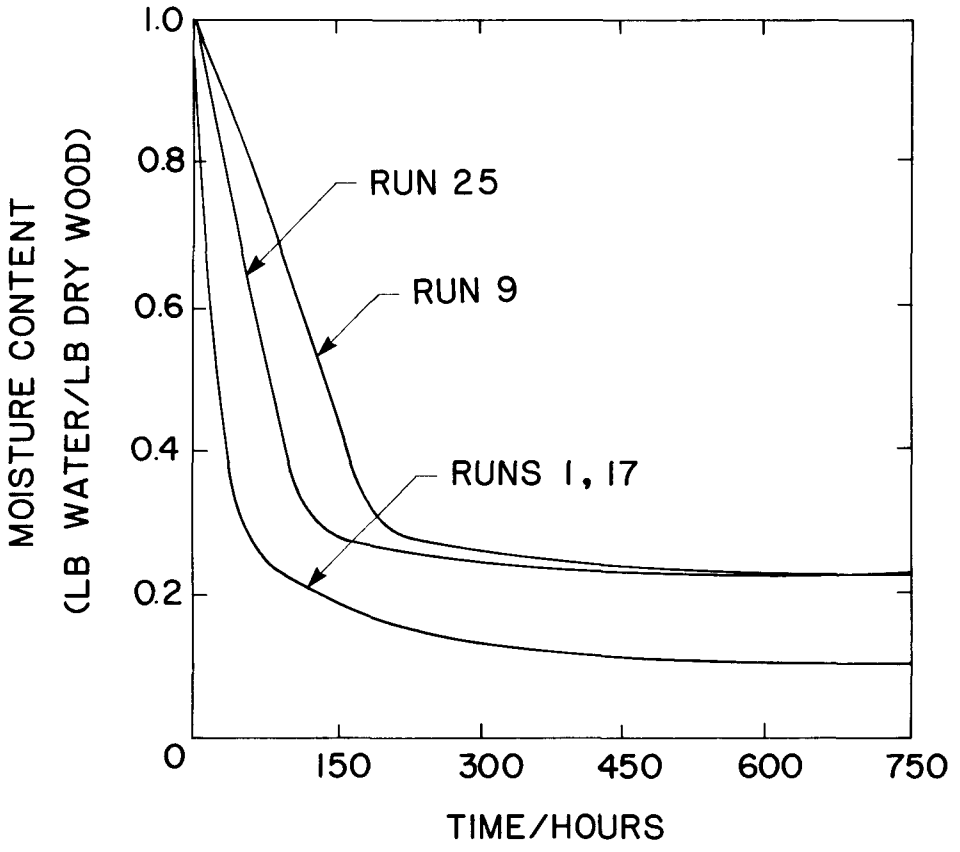

FIG. 1. Average moisture content versus time for runs 1, 9, 17, and 25.

zero moisture content. At an average moisture content of 0.3, the surface of the board is almost at equilibrium moisture content, placing it below the fiber saturation point. The center of the board is still above the fiber saturation point, so the effects of diffusion above and below this point are both important.

For each of the 32 runs, the time to reach an average moisture content of 0.3 was estimated from the plots of average moisture content versus time. These times were recorded and are reported in Table 2. Four typical plots, to which we will make future reference, are illustrated in Fig. 1. As expected, run 12 (thick board, high species factor, low temperature, high humidity, and low air velocity) required the longest of the 32 drying times (659 h). On the other hand, run 21 (thin board, low species factor, high temperature, low humidity, and high air velocity) showed the shortest time (50 h). Run 1 (except for lower temperature) and run 17 (except for lower air velocity) have similar conditions as with run 21 and exhibit about the same drying times.

The moisture profiles in Fig. 2a, 2b, 2c, and 2d correspond to runs 1, 9, 17, and 25 in Fig. 1. In these runs, the thickness, the species factor, and the temperature are held constant at their low levels. As we would expect from the similar drying times, the moisture profiles for runs 1 and 17, taken at 12-h intervals, are almost identical, as shown in Fig. 2a and 2c. The moisture content at the board

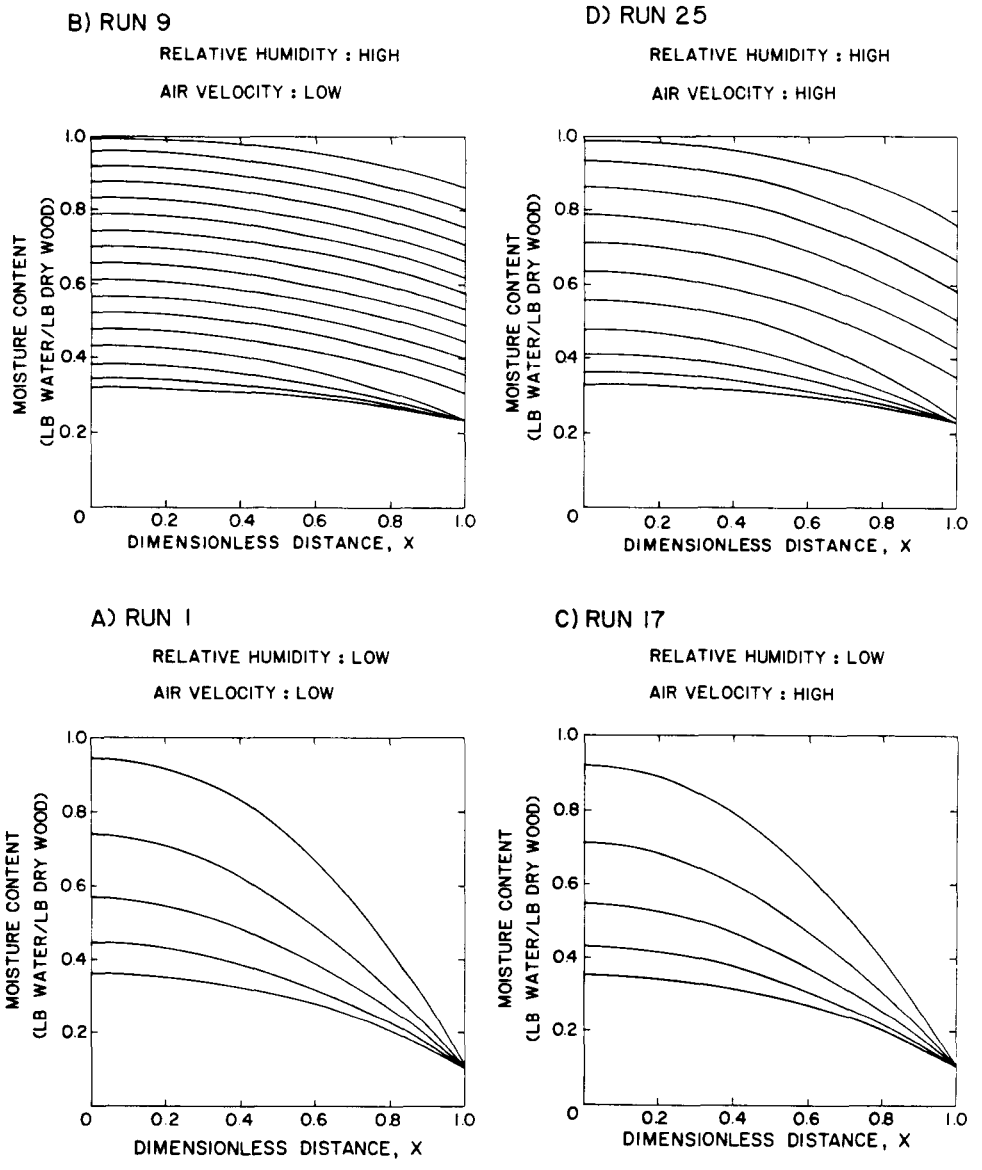

FIG. 2. Moisture profiles at 12-h intervals at low thickness, species factor, and temperature. Relative humidity and air velocity are varied.

surface drops immediately to its equilibrium value of 0.11 lb water/lb dry wood. After this, the rate of moisture movement is controlled entirely by the rate of internal diffusion to the surface. Changing the air velocity has no effect upon the drying rate. The almost equal drying times for runs 1 and 17, 2 and 18, 3 and 19, 4 and 20, 5 and 21, 6 and 22, 7 and 23, and 8 and 24 indicate a similar lack of effect. The corresponding runs at high humidity, i.e., 9 and 25, 10 and 26, 11 and 27, 12 and 28, 13 and 29, 14 and 30, 15 and 31, and 16 and 32, show that air velocity is an important factor as long as the surface moisture content is above

TABLE 3. *Calculated main effects and interaction effects on drying time, based on data in Table 2. The calculated time of an effect is the increase in drying time if the variable, or group of variables, is changed from the low value to the high value. Average time = 230.0 hours.*

Calculated effect or interaction	Value (hours)
A main effect	160.8
B main effect	201.3
C main effect	−51.7
D main effect	133.1
E main effect	−22.2
AB interaction	76.8
AC interaction	−6.9
AD interaction	35.3
AE interaction	−1.7
BC interaction	−5.4
BD interaction	40.6
BE interaction	−0.3
CD interaction	−43.7
CE interaction	18.1
DE interaction	−21.2
ABC interaction	−0.4
ABD interaction	15.1
ABE interaction	1.5
ACD interaction	−4.4
ACE interaction	1.6
ADE interaction	−1.7
BCD interaction	−1.7
BCE interaction	0.6
BDE interaction	0.1
CDE interaction	17.1
ABCD interaction	0.3
ABCE interaction	−1.7
ABDE interaction	0.8
ACDE interaction	1.6
BCDE interaction	0.8
ABCDE interaction	−0.9

A = half-thickness; B = species factor; C = temperature; D = relative humidity; E = air velocity.

equilibrium. In this case, a significant fraction of the overall resistance is external, as a result of the low driving force for evaporation from the surface into the surrounding air. Therefore, there is a slow transition of surface moisture toward the final equilibrium value, as shown in Fig. 2b and 2d. After the moisture content near the surface decreases below the fiber saturation point, the lower diffusion coefficient is used in the model. The internal resistance to mass transfer increases and the surface moisture content becomes constant at its equilibrium value.

The main effect of each variable is the average increase in drying time when that variable changes from its (−) value to its (+) value. All of these, and the effects of interactions between variables, have been calculated and are reported in Table 3. For example, A (thickness) main effect can be interpreted as the additional time required to dry a board if its half-thickness were increased from 0.0417 to 0.0625 ft. The effect was calculated as: A = [average of all results when A = (+) value] − [average of all results when A = (−) value] = 310.4 − 149.6 = 160.8 h. Since the average drying time is 230.0 h, the main effect of A raises the

drying time from 230.0 − ½(160.8) = 149.6 h to 230.0 + ½(160.8) = 310.4 h. Other main effects that show increased times are B (species factor, 201.3 h) and D (relative humidity, 133.1 h). Increase in either thickness or density invariably leads to an increase in drying time because there is more wood substance for moisture to traverse. Increased relative humidity also slows the drying process, because the moisture gradient, which is the driving force for moisture movement and governs the rate of drying, becomes less steep.

The main effects C (temperature) and E (air velocity) show decreased times, −51.7 and −22.2 h, respectively. These effects, however, are not large. The temperature effect is mainly at the board surface, because the edge boundary conditions and the sorption isotherms are functions of temperature. The increase in air velocity from 200 to 600 ft per minute gives a relatively small increase in Reynolds number on the board surface. While this accelerates the mass transfer, the higher velocity still gives a laminar air flow over the board. A significant change in drying rate would not occur unless a turbulent flow pattern developed, which would happen only at an unrealistically high air velocity.

The trends exhibited by the main effects are what we would expect, and show that the model is working as it should.

Predicting drying times would be very simple if the main effects only were important and the variables did not interact. This, unfortunately, is not the case. Variable interaction is observed when the effect of changing one variable depends on the values of one or more of the other variables. As an example, the BD (species factor − relative humidity) interaction is defined as half the difference between the main effect of B, at the high level of D, and the main effect of B, at the low level of D. Thus, the interaction was calculated as:

$$\text{BD interaction} = \frac{[\text{B main effect when D} = (+)\text{ value}]}{2} - \frac{[\text{B main effect when D} = (-)\text{ value}]}{2},$$

which yields 40.6 h. This means the effect of raising the humidity cannot be predicted independent of the species factor. For the less dense species, the humidity main effect is 112.8 h, but for the more dense species, the humidity main effect is 153.4 h.

The largest two-variable interaction was AB (thickness − species factor). The species main effect for the thick board was 278.1 h, but for the thin board it was only 124.5 h, resulting in an interaction of 76.8 h. This interaction exists because internal resistance, caused by a low diffusion coefficient, is more important in thick boards than in thin boards. As shown in Eq. (6), the ratio of the internal and external resistance is proportional to the Sherwood number. Increasing the board thickness makes the external resistance become smaller relative to the internal resistance.

The AD, BD, CD, and DE interactions were all present and significant, probably because of the effect of humidity on the other variables. Of particular interest is the DE (relative humidity − air velocity) interaction. At the high humidity, the air velocity main effect is 43.4 h, but at the low humidity it is only 1.0 h. This

neglible effect of air velocity at low humidity is already described and shown in the moisture profiles of Fig. 2.

The presence of three-variable interactions means that two-variable interactions can depend on the value of a third variable. In the computer model, two of the three-variable interactions, i.e., ABD (thickness-species-humidity) and CDE (temperature-humidity-velocity) interactions were fairly significant. Thus a kiln operator trying to estimate the effect of increasing air circulation must also consider the values of temperature and relative humidity. If he tries to estimate the effect of a change in relative humidity, he needs to account for its interaction with all the other variables. It is now clear why kiln drying has been approached on a trial-and-error basis.

CASE STUDIES

We have applied the same basic model to three practical cases:

Case 1. A conventional dry kiln, with a predetermined temperature and relative humidity schedule.
Case 2. A solar-powered dry kiln, where temperature and relative humidity change on a 24-h cycle during the drying process.
Case 3. A conventional dry kiln, with a predetermined maximum drying rate.

The difference in the model in each of the three cases occurs in the boundary conditions at the surface. It is not constant, but must change during the course of the drying process to meet the conditions imposed either by the desired drying schedule or by the kiln design.

Case 1. Conventional dry kiln model

There are many different kiln schedules, depending largely on the refractory nature of the wood species and the thickness of the board to be dried. For our first case study, we selected constant values that would be fixed by wood species and size, then fixed the air velocity in the kiln. These values are:

Density (green volume basis)	43.0 lb/ft^3
Diffusivity (high)	1.7×10^{-6} cm^2/sec
Diffusivity (low)	0.43×10^{-6} cm^2/sec
Half-thickness	0.0625 ft
Air velocity	200 ft/min

For the temperature and relative humidity schedule we selected the rather mild conditions shown in Fig. 3. The effect of this drying schedule can be seen in the moisture profile. The specific events can be seen more clearly in the moisture profiles in Fig. 4. Initially the temperature is held at 80 F and the relative humidity at 0.9. These conditions are maintained for 8 days. Accordingly, the spacing of the first 16 moisture profiles, taken at 12-h intervals, is rather uniform. That the drying rate is constant can be seen in Fig. 3 by observing the constant slope of that curve over the first 192 h—until the 16th profile.

Lowering the relative humidity to 0.85 for the next 2 days yields a high drying rate, shown by the high slope in Fig. 3 and the wide spacing of moisture profiles 17, 18, 19, and 20 in Fig. 4. It is interesting to note that over the first 12 h of

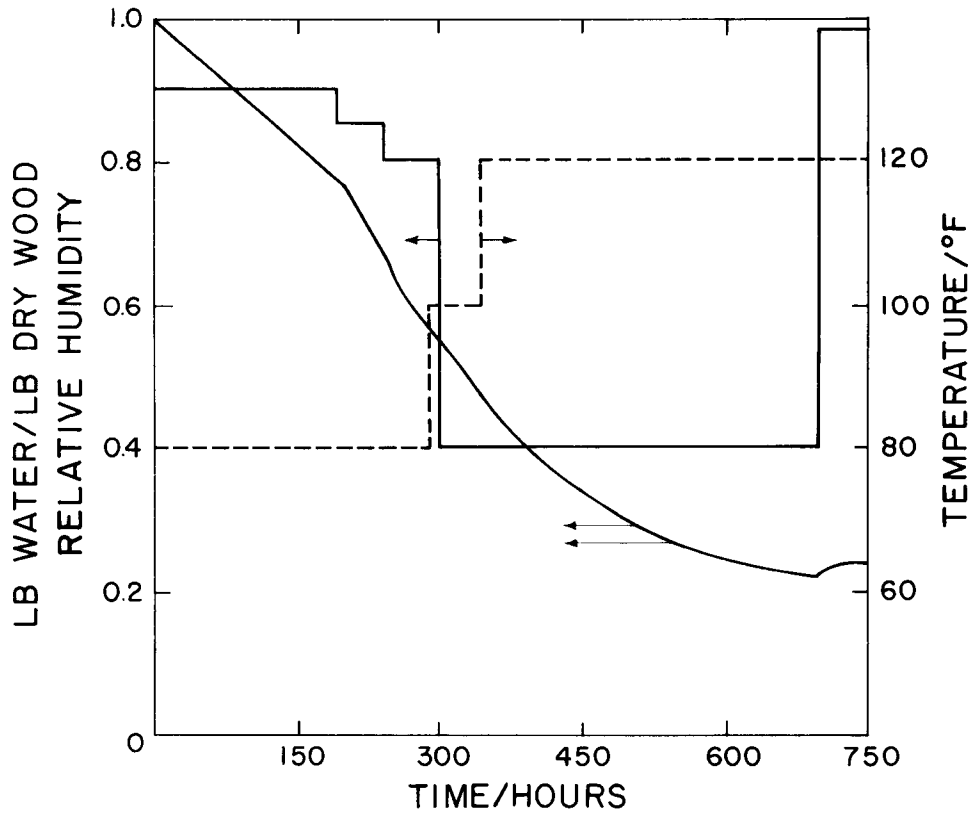

FIG. 3. Relative humidity and temperature schedules (single arrows), and average moisture content (double arrow) for Case Study 1.

this period the effect of the new boundary condition is only exhibited in the 20% of the board nearest the surface. The diffusion process has only carried the effect of the boundary condition that far into the board in 12 h.

Lowering the relative humidity to 0.80 momentarily gives the highest drying rate of all—steepest slope on Fig. 3—beginning at 240 h. Another effect comes into play here as well. The moisture content near the surface of the board has dropped below 0.3 lb water/lb wood. Below this value the model uses the lower diffusion coefficient. Under these conditions of temperature, humidity, and diffusivity, the drying process is controlled entirely by the internal flow of water to the board surface. The (constant) equilibrium moisture content with the surrounding air of 0.21 is maintained at the surface of the board.

The next several events lower the equilibrium moisture content at the surface in successive stages. At 288 h the increase in temperature to 100 F lowers the equilibrium moisture to 0.20. Lowering the relative humidity to 0.4 at 300 h results, a day later (27^{th} profile), in an equilibrium moisture content of 0.075. The lowest surface equilibrium moisture content is 0.065 during the long drying period at a 120 F temperature and 0.4 relative humidity. During this time the drying rate slowly decreases simply because the board has less and less moisture to lose. The moisture profile curves on Fig. 4 get very close together, particularly as the

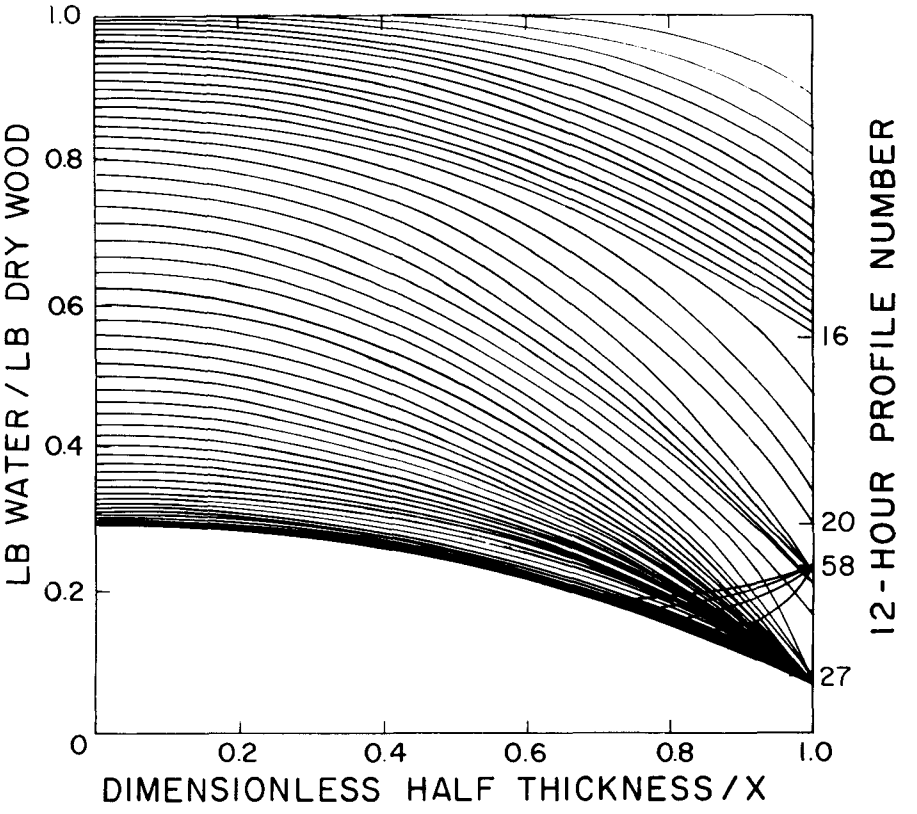

FIG. 4. Moisture profiles at 12-h intervals for Case Study 1.

local concentration decreases below 0.3 and the lower value of diffusivity is used. In Fig. 3, the slope, representing the rate of drying, decreases steadily. It would become flat at a moisture content of 0.065 if the drying continued long enough.

The final change in operating conditions occurs at 646 h (58th profile) and is maintained for 2 days. The relative humidity is increased to 0.98, which, with a temperature of 120 F, gives an equilibrium moisture content of 0.23. Under these conditions moisture reenters the surface of the board, giving a positive slope to the average moisture content in Fig. 3 and a rising sequence to the last four moisture profiles in Fig. 4.

The principal benefit of this first case study is to demonstrate the sensitivity of the model to changes in operating conditions, giving trends we might expect in normal kiln operation.

Case 2. Solar dry kiln model

The temperature and relative humidity, unless supplementary action is taken, vary at the direction of nature, not the kiln operator. Except in cloudy weather, the maximum temperature and minimum humidity coincide in the late afternoon. Similarly, the lowest temperature and highest humidity occur before dawn. These variations can be modeled as sinusoidal functions of time. Therefore, we used the following equations for the model:

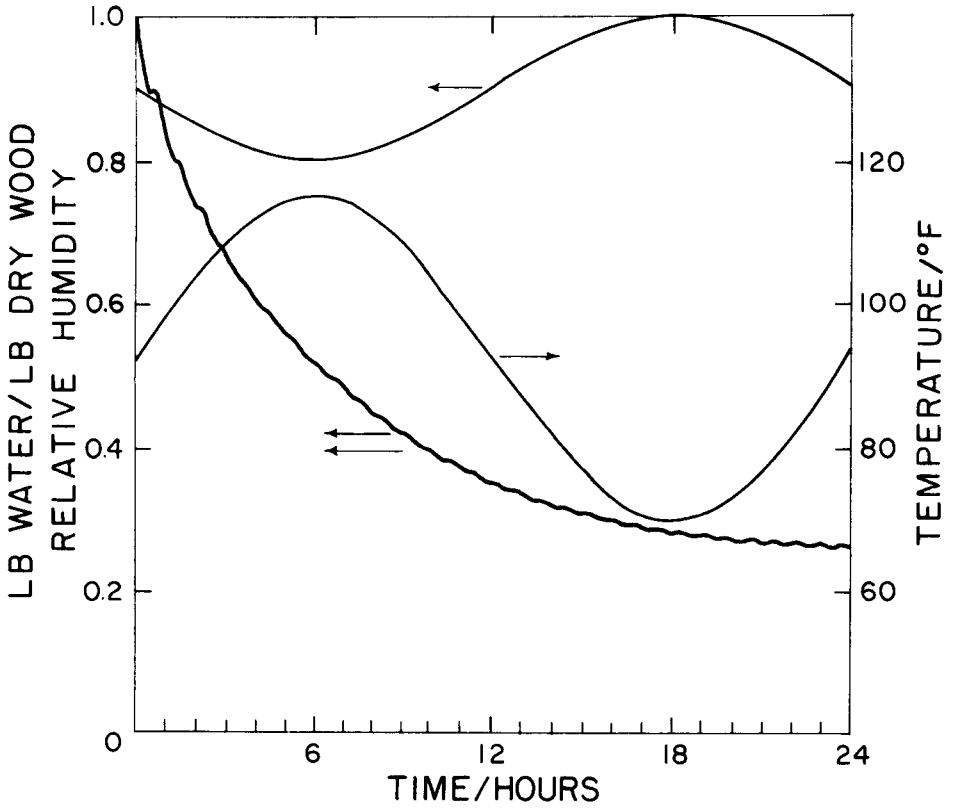

FIG. 5. Daily relative humidity and temperature schedules (single arrows), and average moisture content (double arrow) for Case Study 2.

$$T = 92.5 + 22.5 \ (\sin 2\pi t/24) \tag{10}$$

and

$$RH = 0.9 - 0.1 \ (\sin 2\pi t/24), \tag{11}$$

where t is the drying time in hours. These equations give a temperature range of 70 to 115 F and a relative humidity range of 0.8 to 1.0, as illustrated in Fig. 5. The different signs in front of the sine terms cause the maximum of one function to occur at the same time as the minimum of the other. For the other variables in the model, we have used the same values as in Case Study 1.

The moisture profiles, taken at 12-h intervals, are shown in Fig. 6. Since the profiles cross one another, it is best to look toward the center of the board to find the proper sequence. The first few have been numbered at the right as a further aid. The most favorable drying conditions occur during odd-numbered time periods, peaking at the midpoint of that half cycle, i.e., at 6, 30, 54 h, etc. During even-numbered time periods, the temperature-humidity conditions are such that moisture is readsorbed at the surface of the board. We find, then, that significant drying occurs during the first 12-h time period, with the surface moisture content dropping to 0.31. The slight upward curvature of the profile near the surface indicates that the readsorption of moisture has already began. The surface mois-

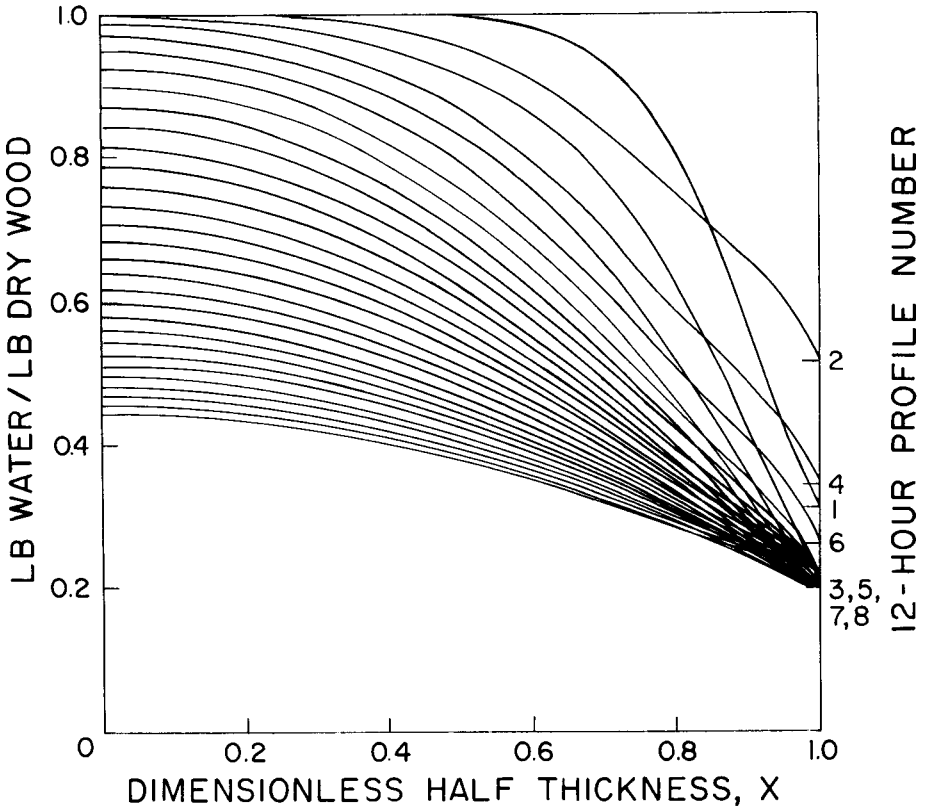

FIG. 6. Moisture profiles at 12-h intervals for Case Study 2.

ture content was below 0.31 an hour or two earlier. During the second 12-h period, enough moisture is readsorbed to raise the surface concentration at the end of 24 h to 0.52. Yet moisture continues to diffuse from deep in the board to replace water lost in the first 12 h. This equalization of moisture content is beneficial because it relieves stresses within the wood.

The cycle of increasing and decreasing surface moisture content continues throughout the drying process. Eventually the wood near the surface of the board dries below the fiber saturation point, 0.3 lb water/lb wood in our case. In this local region, the model employs the local value of the diffusivity. This condition allows the surface of the board to reach equilibrium moisture content with the surroundings in a relatively short time, say less than an hour, compared to the response time at the higher diffusivity. At the end of each 12-h cycle, when the temperature and humidity are again at 92.5 F and 0.9, the surface concentration of the board returns to a moisture content of 0.20. In between these times the surface concentration is higher or lower. This fluctuation is what causes the alternating concave-convex shape of the moisture profiles near the surface.

Throughout the entire process, there are fluctuations in the average moisture content during the 24-h cycle. These are clearly visible in Fig. 5, superimposed on the long-term drying curve. If drying is to proceed for enough time, the average

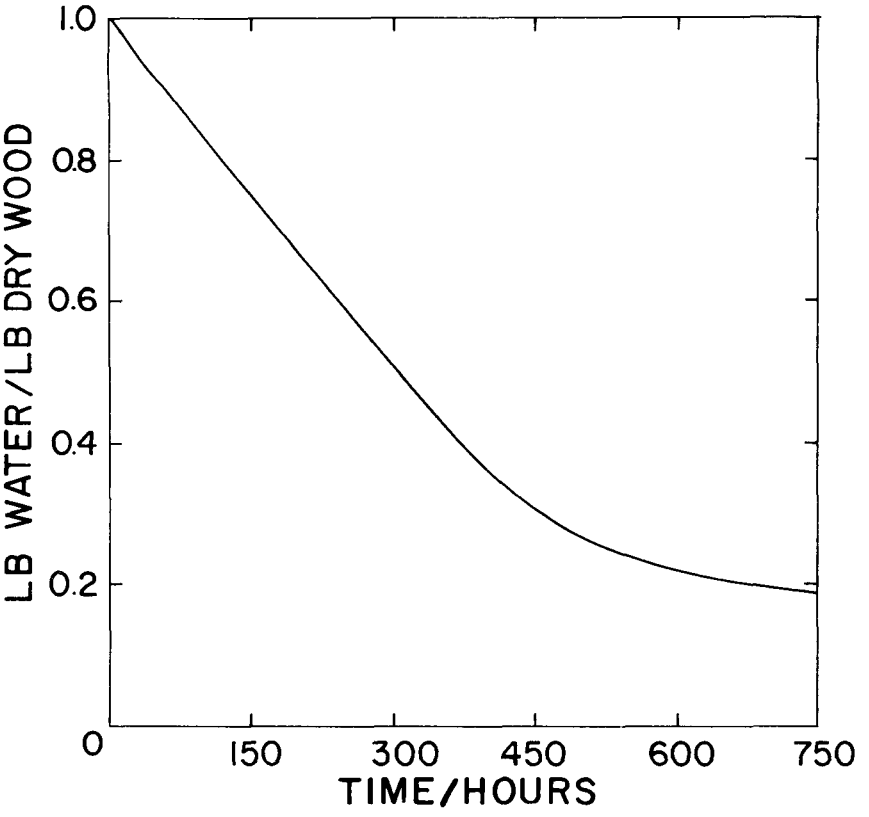

FIG. 7. Average moisture content versus time for Case Study 3.

moisture content will decrease to 0.20, the average surface value, even though it is still 0.26 at the end of 750 h. The final moisture content is thus set by the average conditions during the 24-h cycle.

Case 3. Conventional kiln with predetermined temperature and relative humidity schedule

The computer model can be useful in the development and evaluation of accelerated kiln schedules, especially for the drying of hardwoods where kiln conditions are based on average moisture content of wood. Such schedules are essential for optimizing the drying procedure with automatic programming of drying conditions, which has not yet been successfully accomplished in commercial application with hardwoods.

The model enables us to develop any kind of drying schedule, depending on the desired changes in kiln conditions. In the following illustration the predetermined maximum drying rate is controlled by the daily variation in relative humidity. Temperature and air velocity are held constant for convenience. The procedure is as follows:

1. Select a desired drying rate for a given wood species and thickness for the next time period, which in this study is 24 h.

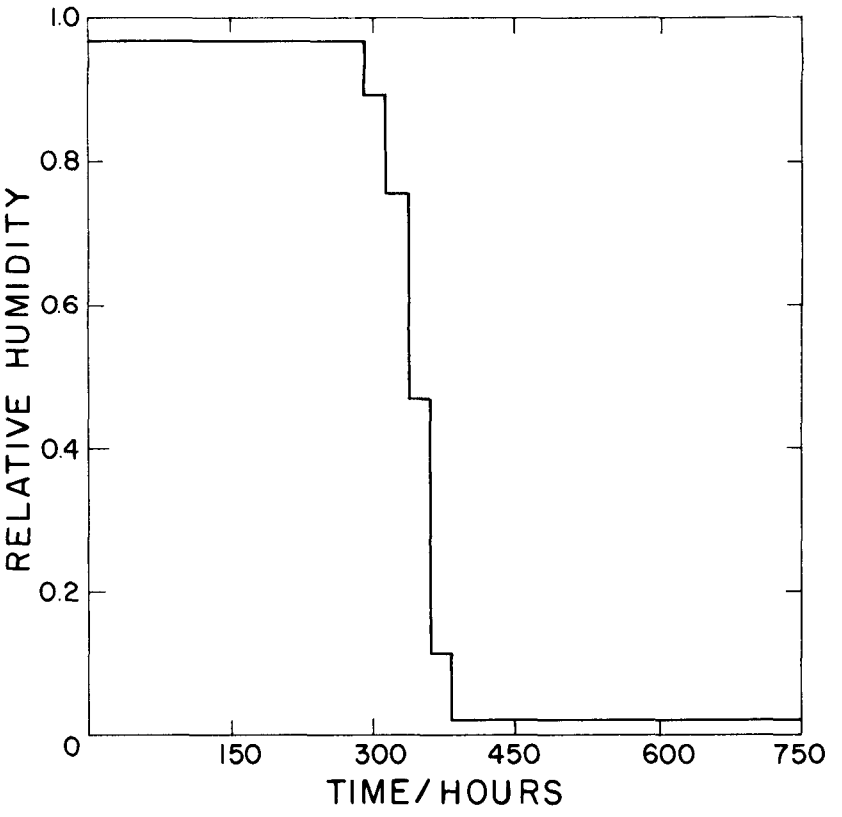

FIG. 8. Computer generated humidity schedule of Case Study 3.

2. "Guess" the relative humidity to achieve the drying rate.
3. Simulate the drying process for 24 h, calculating the drying rate with the computer model.
4. Compare the rate with the desired drying rate in step 1. If the calculated drying rate is not acceptable, back up 24 h and return to step 2.
5. If the drying rate is acceptable, go back to step 1 and select a rate for the next 24 h.

Steps 2–5 are done automatically by the computer, which uses the secant method to generate new "guesses" for the proper relative humidity in step 2. By specifying a list of daily rates in step 1, we can get the computer to generate the correct humidity schedule for any length of time.

For our case study we selected a maximum drying rate of 0.00167 lb water/lb dry wood·h (0.04 lb water/lb dry wood·day). Again, the values used for the other variables are the same as in Case Study 1. Temperature was held constant at 100 F. As shown in Fig. 7 this rate is maintained exactly for some 280 h, and with very little variation for an additional 100 h. The computer generated relative humidity schedule is shown in Fig. 8. For the first 288 h the humidity is held about constant at 0.96. For the next 96 h, the humidity decreases steadily until it reaches a minimum, programmed at 0.02. Thereafter, the drying rate decreases because more severe conditions would be required to maintain it.

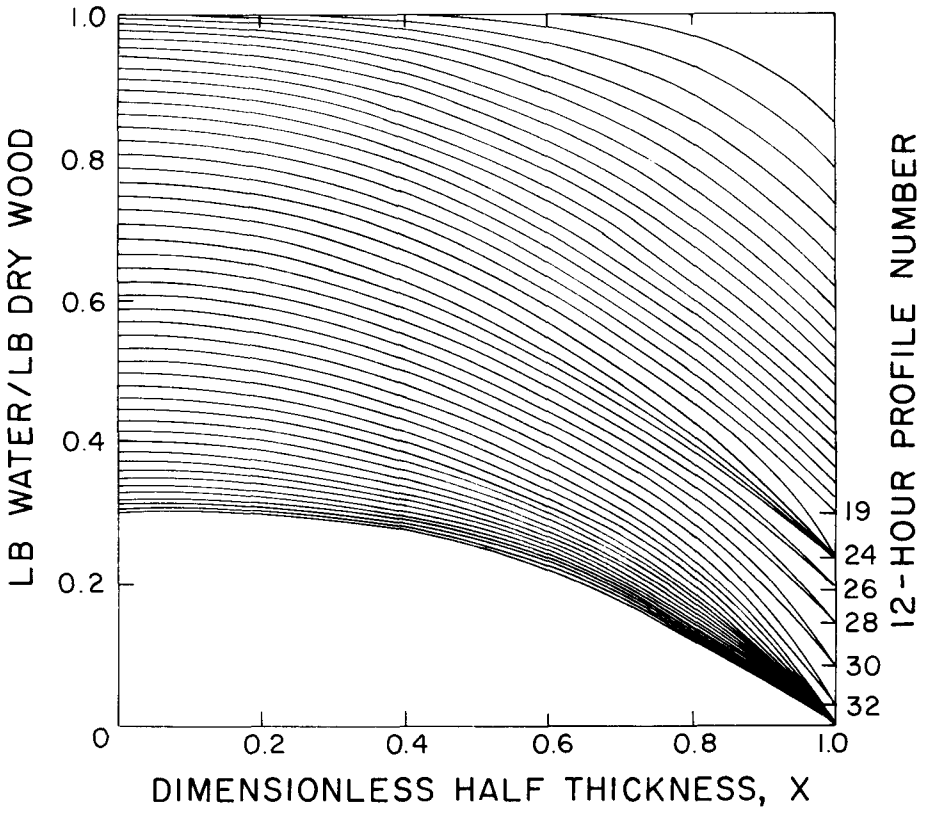

FIG. 9. Moisture profiles at 12-h intervals for Case Study 3.

Figure 9 shows the moisture profiles at 12-h intervals. The first 19 time intervals (228 h) show a steady decrease in moisture content. When the local moisture content near the surface drops below fiber saturation (0.3), the computer program shifts to the lower diffusion coefficient. As in the previous case studies, this causes the major resistance to mass transfer to be inside the board, establishing equilibrium at the surface. Equilibrium is maintained for the next five time intervals at 0.24. At 288 h, the first of five steps of decreasing humidity occurs. Each step, shown in Fig. 8, lasts for 24 h. A new surface equilibrium moisture content is quickly established and maintained for two 12-h periods, as shown in Fig. 9. The final conditions are maintained until the drying process stops at 750 h.

A careful comparison of Figs. 9 and 4 reveals the superiority of the drying schedule of Case Study 3 as compared to Case Study 1. Since large moisture gradients in the wood lead to stresses and defect formation, it is desirable to minimize the gradients. If we take as a measure of the maximum gradient the maximum difference in moisture content between the centerline and the surface, Case Study 3 gives a more favorable result. The maximum difference is 0.52, compared to 0.60 in Case Study 1. This is true even though the ultimate drying conditions of Case Study 3 are more severe and the final moisture content lower. As we noted earlier, casehardening is only caused by large moisture gradients in the wood below fiber saturation. One could adjust the drying conditions to yield

any desired gradient or drying rate. Thus, the operator could dry the lumber at a high rate if all the board is above fiber saturation, then minimize defect formation by controlling the rate below fiber saturation.

CONCLUSIONS

Because of the complexity of wood, any mathematical analysis involves a certain degree of simplifying assumptions. From a microscopic and theoretical viewpoint, the model probably neglects to consider some important factors that may affect wood drying. Nevertheless, from a practical and qualitative viewpoint, the model works very well and reveals information about the wood drying process, namely:

1. It provides drying results for various drying conditions in the kiln.
2. It is useful for developing and evaluating drying schedules, especially when maximum drying rate, or maximum moisture gradient is to be controlled.
3. It could be adapted to other drying situations.

ACKNOWLEDGMENT

This paper was presented at Technical Session 5—Physics—of the 37th Annual Meeting of the Forest Products Research Society, June 20, 1983, in Norfolk, VA. This work was supported in part by the Louisiana Department of Natural Resources under contract No. 21400-81-26.

REFERENCES

ASHWORTH, J. C. 1980. Design of drying schedules for kiln-drying of softwood timber. Developments in drying, vol. 1. Hemisphere Publ. Corp., NY. Pp. 431–442.

BATEMAN, E., J. P. HOHF, AND A. J. STAMM. 1939. Unidirectional drying of wood. Ind. Eng. Chem. 31(9):1150–1154.

BIGGERSTAFF, T. 1965. Drying diffusion coefficients in wood as affected by temperature. For. Prod. J. 15(3):127–133.

BOX, G. E. P., W. G. HUNTER, AND J. S. HUNTER. 1978. Statistics for experimenters. J. Wiley & Sons, NY.

BUI, X., E. T. CHOONG, AND W. G. RUDD. 1980. Numerical methods for solving the equation for diffusion through wood during drying. Wood Sci. 13(2):117–121.

CHOONG, E. T. 1963. Movement of water through a softwood in the hygroscopic range. For. Prod. J. 13(11):489–498.

———. 1965. Diffusion coefficients of softwoods by steadystate and theoretical methods. For. Prod. J. 15(1):21–27.

———, AND C. SKAAR. 1972. Diffusivity and surface emissivity in wood drying. Wood Fiber 4(2): 80–86.

FOREST PRODUCTS LABORATORY, FOREST SERVICE, U.S. DEPARTMENT OF AGRICULTURE. 1974. Wood handbook. Agric. Handbook No. 72., Washington, DC.

GREENHILL, W. L. 1936. The effect of the rate of air circulation on the rate of drying of timber. J. Counc. Sci. & Indus. Res. 9(3):10–15.

HART, C. A. 1964. Principles of moisture movement in wood. For. Prod. J. 14(5):207–214.

KEER, G. A. 1956. Air circulation in the drying kiln. Wood 21(8):314–316.

MAMIT, J. D. 1983. Mechanism of moisture movement in drying hardwoods. M.S. Thesis, School of Forestry and Wildlife Management, Louisiana State Univ., Baton Rouge, LA.

MCNAMARA, W. S., AND C. A. HART. 1971. An analysis of interval and average diffusion coefficient for unsteady-state moisture movement in wood. Wood Sci. 4(1):37–45.

MOSCHLER, W. W., JR., AND R. E. MARTIN. 1968. Diffusion equation solutions in experimental wood drying. Wood Sci. 1(1):47–57.

NADLER, K. C. 1983. Mathematical modeling of the diffusion of water in wood. M.S. thesis, Department of Chemical Engineering, Louisiana State University, Baton Rouge.

NEWMAN, A. B. 1931. The drying of porous solids: Diffusion calculations. Trans. Amer. Inst. Chem. Engin. 27:310–333.

OGURA, T. 1950. Study of wood drying. I. On the relation between the evaporation velocity, the moisture conductivity and the thickness of wood. Rep. Bull. of the Govt. For. Exp. Sta. (Japan), No. 42:1–15. Tokyo (English summary).

PECK, R. E., AND J. Y. KAUH. 1969. Evaluation of drying schedules. AIChE J. 15(1):85–88.

ROSEN, H. N. 1978. The influence of external resistance on moisture adsorption rates in wood. Wood Fiber 10(3):218–228.

SALAMON, M. 1960. Air circulation in dry kilns. Proc. Ann. Meeting of Wester Dry Kiln Clubs, Missoula, MT, June 23–24, 1960.

SIAU, J. F. 1980. Nonisothermal moisture movement in wood. Wood Sci. 13(1):11–13.

SKAAR, C. 1954. Analysis of methods for determining the coefficient of moisture diffusion in wood. For. Prod. J. 4(6):403–410.

SPOLEK, G. A., AND O. A. PLUMB. 1980. A numerical model of heat and mass transport in wood during drying. Proc. 2nd International Drying Symposium, vol. 2, Montreal, Canada, Hemisphere Publ. Corp., NY. Pp. 84–92.

STAMM, A. J. 1964. Wood and cellulose science. Ronald Press, NY.

STRAMM, A. I., AND R. M. NELSON, JR. 1961. Comparison between measured and theoretical drying diffusion coefficients for southern pine. For. Prod. J. 11(11):536–543.

VICK, C. B. 1965. Drying-rate curves for one-inch yellow poplar lumber in low-temperature forced-air dryers. For. Prod. J. 15(12):500–504.

YAO, J. 1966. A new approach to the study of drying diffusion coefficients in wood. For. Prod. J. 16(6):61–69.